European Journal of Nuclear Medicine and Molecular Imaging (2023) 50:2271–2281
https://doi.org/10.1007/s00259-023-06207-2

ORIGINAL ARTICLE

One-stop [^{18}F]FDG and [^{68}Ga]Ga-DOTA-FAPI-04 total-body PET/CT examination with dual-low activity: a feasibility study

Guobing Liu[1,2,3,4] · Wujian Mao[1,2,3,4] · Haojun Yu[1,2,3,4] · Yan Hu[1,2,3,4] · Jianying Gu[5] · Hongcheng Shi[1,2,3,4]

Received: 19 November 2022 / Accepted: 18 March 2023 / Published online: 27 March 2023

Abstract

Purpose Positron emission tomography/computed tomography (PET/CT) based on fibroblast activation protein inhibitors (FAPI) has shown complementary values to 2-[^{18}F]-fluoro-2-deoxy-D-glucose ([^{18}F]FDG) in cancer imaging. This study aimed to investigate the feasibility of a one-stop FDG-FAPI dual-tracer imaging protocol with dual-low activity for oncological imaging.

Methods Nineteen patients with malignancies underwent one-stop [^{18}F]FDG (0.37 MBq/kg) PET (PET_{FDG}) and dual-tracer PET 30–40 and 50–60 min (hereafter, $PET_{D30–40}$ and $PET_{D50–60}$, respectively) after additional injection of [^{68}Ga]Ga-DOTA-FAPI-04 (0.925 MBq/kg), with a single diagnostic CT to generate the PET/CT. The lesion detection rate and tumor-to-normal ratios (TNRs) of tracer uptake were compared between PET_{FDG}/CT and $PET_{D50–60}$/CT and between $PET_{D50–60}$/CT and $PET_{D30–40}$/CT. In addition, a visual scoring system was established to compare the lesion detectability.

Results The dual-tracer $PET_{D50–60}$ and $PET_{D30–40}$/CT showed similar performance in detecting primary tumors but presented significantly higher lesion TNRs than PET_{FDG}. Significantly, more metastases with higher TNRs were identified on $PET_{D50–60}$ than PET_{FDG} (491 *vs.* 261, $P<0.001$). The dual-tracer $PET_{D50–60}$ received significantly higher visual scores than single PET_{FDG} (111 *vs.* 10) in demonstrating both primary tumors (12 *vs.* 2) and metastases (99 *vs.* 8). However, these differences were not significant between $PET_{D50–60}$ and $PET_{D30–40}$. These resulted in tumor upstaging in 44.4% patients taking PET/CT for initial assessment, and more recurrences (68 *vs.* 7) were identified in patients taking PET/CT for restaging, both on $PET_{D50–60}$ and $PET_{D30–40}$, compared to PET_{FDG}. The reduced effective dosimetry per patient (26.2 ± 2.57 mSv) was equal to that of a single standard whole-body PET/CT.

Conclusion The one-stop dual-tracer dual-low-activity PET imaging protocol combines the strengths of [^{18}F]FDG and [^{68}Ga]Ga-DOTA-FAPI-04 with shorter duration and lesser radiation and is thus clinically applicable.

Keywords 2-[^{18}F]-Fluoro-2-deoxy-D-glucose ([^{18}F]FDG) · Fibroblast activation protein inhibitor (FAPI) · Positron emission tomography/computed tomography (PET/CT) · Dual-tracer imaging

Introduction

Fibroblast activation protein (FAP) is overexpressed by cancer-associated fibroblasts (CAFs) of the tumor stroma, and their activation is closely associated with tumor progression [1]. In recent years, many quinolone-based FAP inhibitors (FAPI) have been fabricated as PET tracers for cancer imaging [2], of which [^{68}Ga]Ga-FAPI-04 is very promising for PET imaging of various cancers [3–5]. However, many limitations of FAPI-based imaging remain unaddressed. For example, FAPI expression occurs not only in malignancies but also in stromal remodeling of chronic inflammation, wound healing, and certain physiologic processes, causing challenges for tumor diagnosis in FAPI imaging [2]. In addition, FAPI-based PET is still controversial in diagnosing lymph-node metastases in different tumors and in diagnosing

Guobing Liu and Wujian Mao contributed equally to this study.

This article is part of the Topical Collection on Miscellanea

✉ Jianying Gu
gu.jianying@zs-hospital.sh.cn

✉ Hongcheng Shi
shi.hongcheng@zs-hospital.sh.cn

1 Department of Nuclear Medicine, Zhongshan Hospital, Fudan University, Shanghai, China

2 Institute of Nuclear Medicine, Fudan University, Shanghai, China

3 Shanghai Institute of Medical Imaging, Shanghai, China

4 Cancer Prevention and Treatment Center, Zhongshan Hospital, Fudan University, Shanghai, China

5 Department of Plastic Surgery, Zhongshan Hospital, Fudan University, Shanghai, China

primary colorectal and pancreatic cancers combined with chronic inflammation [6–8]. Changes of microenvironment in tumor development may lead to changes in the expression of FAP, so whether different aspects of tumor variability have an impact on FAPI imaging results needs further exploration. Therefore, FAPI-based PET/CT cannot yet replace the role of FDG PET/CT, but often run as a complement to it.

For over 40 years, [^{18}F]FDG has been the dominant PET tracer particularly in tumor imaging, representing the current gold standard. Given the different targeting component of tumors from the parenchyma to stroma, a combination of [^{68}Ga]Ga-FAPI PET and [^{18}F]FDG PET has shown complementary clinical value [3–5]. However, most of these studies were performed on two different days, which resulted in prolonged duration and increased radiation exposure to patients. Recently, a single-day dual-tracer imaging protocol was proposed by Roth et al. which dramatically reduced time cost, but could not solve the radiation exposure problem [9].

In recent years, the improved sensitivity of the PET system with long axial field of view (AFOV) including the "uEXPLORER" (United Imaging Healthcare, Shanghai, China) [10] and the "Quadra" (Siemens Healthineers, Knoxville, USA) [11] has enabled PET imaging with low tracer activity [11, 12] and delayed imaging time [13]. These advantages also make PET imaging more convenient to be performed with low radiation, which is of particular concern for dual-tracer imaging. By using the total-body PET/CT scanner, we proposed a one-stop FDG-FAPI dual-tracer, dual-low-activity imaging protocol with a single CT scan to reduce radiation from both radionuclides and CT. The aim of this study was to investigate the feasibility of this protocol for cancer imaging.

Materials and methods

Patient enrollment

This single-center prospective study was approved by the Review Board (B2022-098R2) of our hospital. Written informed consent was obtained from all patients. Patients were consecutively recruited from August 2022 to October 2022. All patients received the first [^{18}F]FDG PET/CT and then FAPI-weighted PET/CT after additional injection of [^{68}Ga]Ga-FAPI-04 immediately after the [^{18}F]FDG PET/CT scan. We selected this imaging protocol to mainly ensure the basic requirement of PET imaging ([^{18}F]FDG PET) first and then considered the complementary FAPI-weighted PET imaging, since [^{18}F]FDG PET is still the gold standard of clinical PET imaging. The inclusion criteria were as follows: (a) patients with suspected or confirmed malignancies, (b) patients whose general status was stable and those who agreed to undergo paired [^{18}F]FDG and dual-tracer PET/CT, and (c) patients who provided informed consent. The exclusion criteria were as follows: (a) patients with nonmalignant disease, (b) those without confirmed pathological diagnosis, and (c) pregnant patients. The pathological results of patients were obtained by reviewing medical records before PET/CT examination or by a one-month follow-up carried out after PET/CT examination.

Preparation of [^{18}F]FDG and [^{68}Ga]Ga-DOTA-FAPI-04

[^{18}F]FDG was manufactured in accordance with the standard method in our institution using the [^{18}F]FDG synthesis module (PET-FDG-IT-NA, PET Technology Co., Ltd., Beijing, China). The FAPI precursor—1,4,7,10-tetraazcylododecane-1,4,7,10-tetraaceticacid (DOTA) containing FAPI-04—was purchased from Huayi Technology Co., Ltd. (Jiangsu, China). Radiolabeling of DOTA-FAPI-04 was conducted by adding 1 mL 0.25 M sodium acetate and 4 mL ^{68}Ga solution (370 MBq in 0.05 M HCl) to 100 µg DOTA-FAPI-04. The reaction mixture was heated to 95 °C for 10 min. The final pH was around 6.0. Radio-high-performance liquid chromatography (R-HPLC) showed that the radiochemical yields of both [^{18}F]FDG and [^{68}Ga]Ga-DOTA-FAPI-04 were above 90%. Finally, both [^{18}F]FDG and [^{68}Ga]Ga-DOTA-FAPI-04 were diluted with saline and sterilized by passing through a 0.22-µm Millipore filter into a sterile syringe. The radiochemical purity of [^{18}F]FDG and [^{68}Ga]Ga-DOTA-FAPI-04 was both above 98%, confirmed by R-HPLC.

PET/CT acquisition

After patients had fasted for 6 h and had their glycemia tested (range: 5.0–6.9 mmol/L), an injection of ultralow activity [^{18}F]FDG (0.37 MBq/kg), defined as one-tenth of the standard full activity (3.7 MBq/kg), was administered, based on our previous experiences [14]. Approximately 84.6 ± 28.0 min later, total-body PET/CT was performed using the uEXPLORER scanner. A low-dose CT (5–10 mAs, 120 kV) was first performed for attenuation correction (AC). Then, diagnostic free-breathing CT was performed using the following parameters: modulated tube current and tube voltage of 120 kV for the body and 258 mAs and 120 kV for the head; collimation, 64×0.5 mm; pitch, 1.0; and matrix, 512×512. Static PET was acquired for 10 min and reconstructed into a slice thickness of 1.443 mm using the ordered-subset expectation maximization algorithm with three iterations, 20 subsets, and a matrix of 192×192. Immediately following the [^{18}F]FDG PET/CT scan, a 60-min dynamic PET scanning was performed with the patient's position unchanged after injection of half-activity [^{68}Ga]Ga-DOTA-FAPI-04 (0.925 MBq/kg) based on previous studies [3–5]. Static PET (FAPI-weighted) using the data of

30–40 and 50–60 min (hereafter, $PET_{D30–40}$ and $PET_{D50–60}$, respectively) was reconstructed with the same parameters as [^{18}F]FDG PET (PET_{FDG}). Both the PET_{FDG} and the dual-tracer PET used the same AC CT and diagnostic CT to generate integrated PET/CT for analysis. The imaging protocol is illustrated in Fig. 1. Any complaint regarding adverse events from patients during the PET/CT scan was recorded by one of the authors (W.M.). In addition, this was checked immediately and 30 min after the whole examinations.

Imaging review

Two nuclear medicine physicians (with 3 and 6 years' board-certified experience, respectively) independently reviewed the [^{18}F]FDG PET/CT and dual-tracer PET/CT in random order. Any difference in opinion was resolved by consensus. Diagnostic CT was used for correlation and for the purpose to exclude unspecific findings.

On PET images, lesions were positive if the tracer uptake exceeded that of the adjacent background tissues accompanied by abnormalities on CT, when the possibility of nonspecific findings could be excluded. For lesions in areas where no obvious tracer uptake could be observed (e.g., mesenteric fat), the adjacent normal muscle was selected as the reference organ. Lesions were classified as primary and metastatic. Lymph-node metastases were divided into neck/supraclavicular, mediastinal (including the hilum lymph node), abdominal, and pelvic (including inguinal lymph node). Peritoneal metastases were classified into either nodular or diffuse type, and the extent was assessed according to Sugarbaker's 13 regions [15]. In addition, the maximum tracer concentration (TC_{max}) of lesions (Bq/mL) was measured. For diffuse-type peritoneal metastases, only TC_{max} was recorded, while for nodular-type peritoneal metastases and lesions in other places, both TC_{max} and size were measured. For reference tissues, mean TC was measured within a spherical volume of interest of 3-cm diameter in the right liver and of 1-cm diameter in the ascending aorta (blood pool). Then, the tumor-to-normal ratio (TNR) of lesions, including tumor-to-liver ratio (TLR) and tumor-to-blood ratio (TBR), was calculated by dividing the TC_{max} of lesions with the mean TC of the liver and blood pool, respectively.

In addition, a visual scoring system was established to compare the lesion detection capabilities, based on the area, number, and tracer uptake of lesions, according to the method described in a previous study [16]. If the area/number/tracer uptake of lesions detected by $PET_{D50–60}$ was 1–3, 3–5, or > 5 times more than that of PET_{FDG}, $PET_{D50–60}$ was scored as 1, 2, and 3, respectively, whereas the PET_{FDG} was scored as 1, 2, and 3, if the area/number/tracer uptake of lesions detected by PET_{FDG} was 1–3, 3–5, or > 5 times more than that of $PET_{D50–60}$, respectively. Otherwise, the score was 0. The same criterion was used to compare the lesion detection capabilities between $PET_{D30–40}$ and $PET_{D50–60}$.

Clinical staging of patients

For treatment-naive patients, the clinical TNM stage was assigned based on the eighth edition of the American Joint Committee on Cancer staging system independently after [^{18}F]FDG PET/CT and dual-trace PET/CT imaging [17].

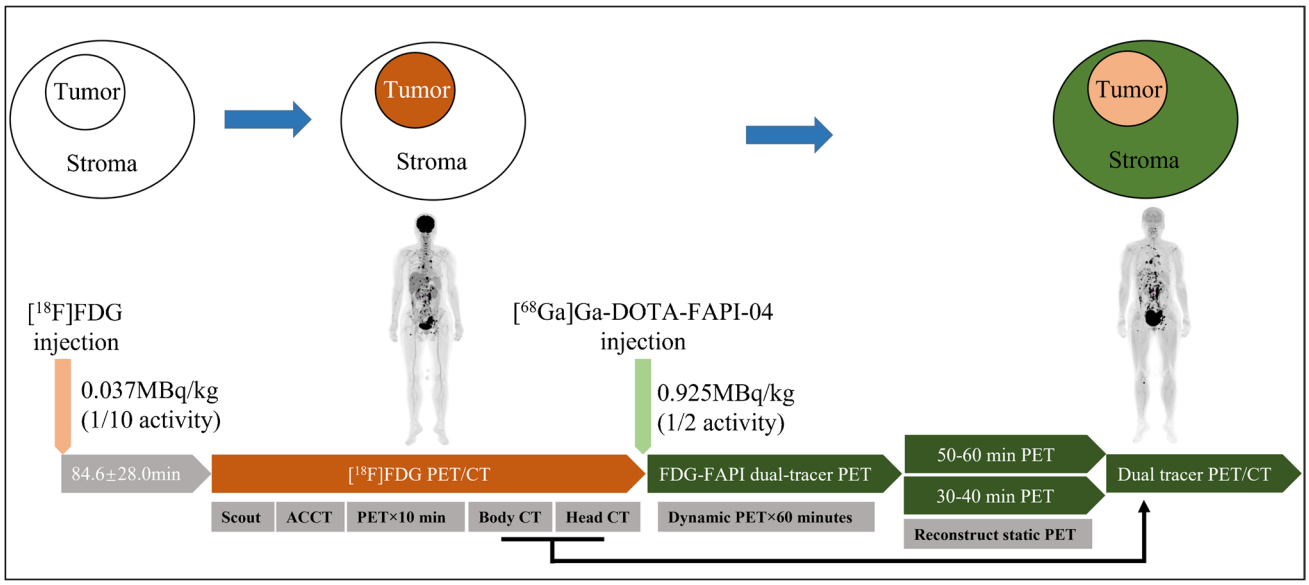

Fig. 1 Schematic diagram of the imaging protocol. This figure was adapted with permission from a JNM article—Roth KS, Voltin CA, van Heek L, etal. J Nucl Med 2022; 63(11):1683-1686. © SNMMI (ref. 9).

Dosimetry estimation

Radiation dosimetry was calculated by adding the effective dose of [^{18}F]FDG, [^{68}Ga]Ga-DOTA-FAPI-04, and CT. The dose of [^{18}F]FDG was briefly calculated as 0.019 mSv/MBq × injected activity (MBq) according to the ICRP Publication 106 [18], and the dose of [^{68}Ga]Ga-DOTA-FAPI-04 was calculated as 0.0164 mSv/MBq × injected activity (MBq) according to the results of a previous study [19]. The dose of CT including scout, ACCT, body CT, and head CT was calculated by multiplying the dose length product (mGy·cm) with the ICRP conversion coefficient as 0.015 mSv/(mGy·cm) [20].

Statistical analysis

Statistical analyses were conducted using SPSS 20 (IBM Corporation, NY, USA) with two-sided $P < 0.05$ indicating statistical significance. Comparisons of lesion detectability among different PET sets were performed using the Cochran Q test. For comparisons of quantitative indices among different PET sets, one-way ANOVA with repeated measures or the Freidman test was used depending on the normality of variables confirmed by the Kolmogorov–Smirnov test. The Bonferroni corrections were applied for the pairwise post hoc comparisons.

Results

Basic information

Twenty-one patients received the [^{18}F]FDG PET/CT and dual-tracer PET/CT without any reported side effects or adverse events. One patient with multiple metastases on admission refused to perform biopsy and was excluded because no pathological result could be obtained. Another patient was excluded because of poor image quality of the dual-tracer PET caused by injection leakage when performing injection of [^{68}Ga]Ga-DOTA-FAPI-04. The flowchart of patient enrollment is presented in Fig. 2. Finally, 19 patients were included for analysis. The aims of the PET/CT studies were for initial diagnosis/staging in eight patients, for recurrence detection (restaging) in four patients, and for therapy response evaluation in seven patients. Among these patients, 11 (57.9%) had gastric cancer, 2 (10.5%) had ovarian cancer, 2 (10.5%) had cervical cancer, 2 (10.5%) had colon cancer, and 1 (5.3%) patient each had laryngeal cancer and appendiceal cancer. One patient had synchronous primary cervical cancer and intestinal neuroendocrine tumor. Patients' basic information is summarized in Table 1.

Comparison of lesion detection and quantitative assessments

A total of nine primary tumors were identified, all of which were detected both on PET_{FDG}, $PET_{D50–60}$, and $PET_{D30–40}$ PET (9/9 *vs.* 9/9 *vs.* 9/9, Table 2). However, the tracer uptake, in terms of TLR (11.45 ± 5.92 *vs.* 4.27 ± 3.14, $P = 0.028$) and TBR (12.71 ± 6.44 *vs.* 6.51 ± 4.69, $P = 0.035$), was significantly higher on $PET_{D50–60}$ than that on PET_{FDG} (Figs. 3, 4, and 5), but comparable to that on $PET_{D30–40}$ (Table 2). A total of 491 metastases were suspected on $PET_{D50–60}$, significantly higher than that on PET_{FDG} (261, $P < 0.001$). Specifically, significantly more metastases in the lymph nodes (257 *vs.* 121, $P < 0.001$; Fig. 3), peritoneum (132 *vs.* 63, $P < 0.001$; Fig. 4), and liver (45 *vs.* 20, $P < 0.001$; Fig. 5) were found on $PET_{D50–60}$ than on PET_{FDG}. However, these results were the same between $PET_{D50–60}$ and $PET_{D30–40}$. Dual-tracer PET performed equally in exploring metastases

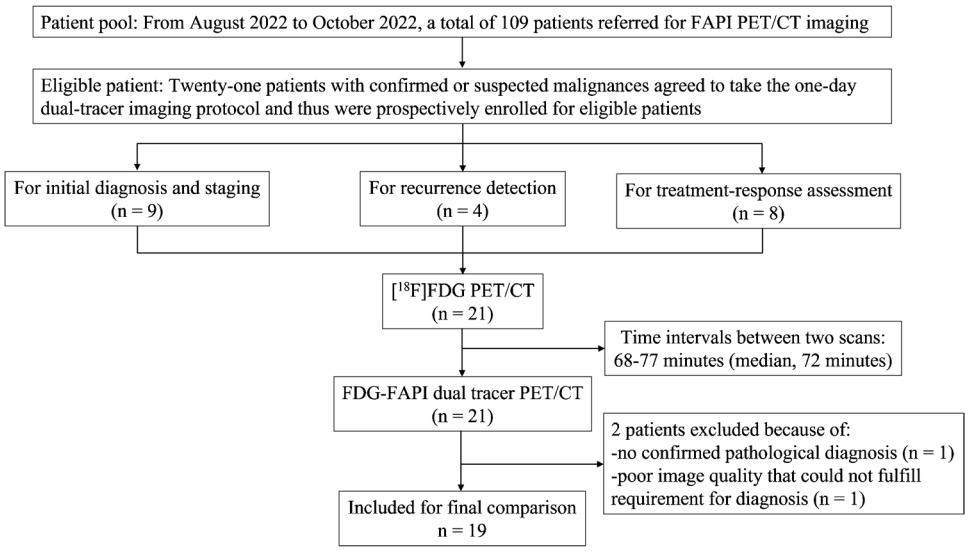

Fig. 2 Flowchart of patient enrollment

Table 1 Basic and clinical information of the 19 patients included in this study

Characteristics	$N = 19$
Sex,*n*(%)	
Male	8 (42.1%)
Female	11 (57.9%)
Age, years (mean ± SD)	59.2 ± 13.8
Glycemia, mmol/L, mean (range)	5.8 (5.0–6.9)
Method of final diagnosis	
Biopsy,*n*(%)	3 (15.8%)
Surgery,*n*(%)	16 (84.2%)
Tumors*,*n*(%)	
Gastric cancer	11 (57.9%)
Ovarian cancer	2 (10.5%)
Cervical cancer	2 (10.5%)
Colon cancer	2 (10.5%)
Laryngeal cancer	1 (5.3%)
Intestinal neuroendocrine tumor	1 (5.3%)
Appendiceal cancer	1 (5.3%)
Indications for PET/CT,*n*(%)	
Initial assessment (diagnosis/staging)	8 (42.1%)
Recurrence detection (restaging)	4 (21.1%)
Therapy response evaluation	7 (36.8%)
Tracer injection	
[^{18}F]FDG, MBq (mean ± SD)	22.8 ± 6.8
[^{68}Ga]Ga-DOTA-FAPI-04, MBq (mean ± SD)	54.4 ± 9.8
Time between [^{18}F]FDG injection and scan (min)	84.6 ± 28.0
Time between [^{18}F]FDG and FAPI injection (min)	112.2 ± 29.6

SD standard deviation

*The summed percentage of all types exceeded 100%, because one patient had synchronous primary cervical cancer and intestinal neuroendocrine tumor

in the bone (29 *vs.* 28) and the lung (28 *vs.* 28), when compared to PET_{FDG}. All metastases presented significantly higher TLRs on $PET_{D50–60}$ than on PET_{FDG}, but were similar to those on $PET_{D30–40}$. In lymph-node metastases, the advantage of dual-trace imaging over single-trace imaging was more obvious in lesions with diameter < 1 cm (221 *vs.* 94, $P < 0.001$) than in lesions with diameter ≥ 1 cm (36 *vs.* 27, $P = 0.004$).

Comparison of visual evaluation

Compared to PET_{FDG}, $PET_{D50–60}$ received a dramatically higher total visual score (111 *vs.* 10, Fig. 6A). Specifically, dual-tracer $PET_{D50–60}$ detected significantly more or larger lesions than PET_{FDG} in the primary tumors (12 *vs.* 2) and in metastases from the lymph nodes (59 *vs.* 3), peritoneum (21 vs. 0), ovaries (3 *vs.* 1), liver (7 *vs.* 0), and bone (9 *vs.* 4). However, compared to PET_{FDG}, dual-tracer $PET_{D50–60}$ showed no advantage in detecting metastases in the lung (0 *vs.* 0). The visual scores of $PET_{D50–60}$ and $PET_{D30–40}$ were quite similar (21 *vs.* 14, Fig. 6B).

Comparisons of initial assessment and recurrence detection

Regarding the eight patients with nine primary tumors taking PET/CT for initial assessment, upstaging was found in 4 (44.4%) patients after dual-tracer PET/CT, compared with [^{18}F]FDG PET/CT (Table 3). As for patients taking PET/CT for recurrence detection, recurrences were demonstrated in all four patients with 68 lesions identified by both $PET_{D50–60}$ and $PET_{D30–40}$, while only three patients with seven lesions were revealed by PET_{FDG}.

Dosimetry

The total effective radiation dose of patients was about 26.22 ± 2.57 mSv (Table 4), which was largely resulted from CT scan (24.89 ± 2.37 mSv) and less caused by [^{18}F]FDG- or [^{68}Ga]Ga-DOTA-FAPI-04-imparted radiation (0.43 ± 0.13 mSv and 0.89 ± 0.16 mSv, respectively).

Discussion

In this work, we investigated the feasibility of [^{18}F]FDG/[^{68}Ga]Ga-DOTA-FAPI-04 dual-tracer, dual-low-activity PET/CT for oncological imaging. The dual-tracer PET presented obvious advantages over single [^{18}F]FDG PET in lesion detection and visual assessment including lesion number, extent, and tracer uptake. These advantages resulted in tumor upstaging in 44.4% (4/9) patients who underwent PET/CT for initial assessment, and more recurrent lesions (68 *vs.* 7) were detected in more patients (4 *vs.* 3) that underwent PET/CT for restaging. In addition, the advantages of dual-tracer PET can be obtained with reduced acquisition time to 30 min post additional injection of [^{68}Ga]Ga-DOTA-FAPI-04.

We believe that the results of our study have clinical significance. Given the many promising results in cancer imaging, ^{68}Ga-FAPI PET appears complementary to [^{18}F]FDG PET [2–5]. However, most of these two PET/CT scans were performed in two days, which was undoubtedly inconvenient and resulted in extra radiation exposure to patients. The one-stop imaging protocol in the current study reduced the overall time required. In addition, this protocol avoided a whole-body diagnostic CT scan, which produced the main radiation of PET/CT (24.89 ± 2.37 mSv). Accompanied by the dual-low activity of injected [^{18}F]FDG and [^{68}Ga]Ga-DOTA-FAPI-04, the total effective dosimetry (26.22 ± 2.57 mSv) was equal to that of a single standard whole-body [^{18}F]FDG PET/CT scan (21–32 mSv) reported

Table 2 Comparisons of lesion detection and quantification between [^{18}F]FDG and FDG-FAPI dual-tracer PET/CT imaging

Lesions	Positive detection (*n*)			TLR (mean ± SD)			TBR (mean ± SD)		
	PET_{FDG}	PET_{D50-60}	PET_{D30-40}	PET_{FDG}	PET_{D50-60}	PET_{D30-40}	PET_{FDG}	PET_{D50-60}	PET_{D30-40}
Primary tumors	9 (> 0.999*)	9	9 (> 0.999*)	4.27 ± 3.14 (0.028†)	11.45 ± 5.92	11.97 ± 6.24 (0.426†)	6.51 ± 4.69 (0.035†)	12.71 ± 6.44	13.28 ± 6.94 (0.574†)
Metastasis	261 (< 0.001*)	491	491 (> 0.999*)	1.81 ± 1.51 (< 0.001‡)	5.37 ± 3.65	5.25 ± 3.37 (0.310‡)	2.79 ± 3.39 (< 0.001‡)	5.70 ± 3.56	5.56 ± 3.27 (0.237‡)
LN (total)	121 (< 0.001*)	257	257 (> 0.999*)	1.39 ± 1.06 (< 0.001‡)	5.20 ± 3.18	5.18 ± 3.08 (0.852‡)	2.16 ± 1.72 (< 0.001‡)	5.57 ± 2.98	5.50 ± 2.82 (0.502‡)
≥ 1 cm	27 (0.004*)	36	36 (> 0.999*)	2.32 ± 1.66 (< 0.001‡)	7.40 ± 5.11	7.10 ± 4.89 (0.126‡)	3.92 ± 2.97 (< 0.001‡)	7.76 ± 4.49	7.40 ± 4.11 (0.231‡)
< 1 cm	94 (< 0.001*)	221	221 (> 0.999*)	1.24 ± 0.84 (< 0.001‡)	4.84 ± 2.59	4.87 ± 2.56 (> 0.999‡)	1.87 ± 1.19 (< 0.001‡)	5.20 ± 2.49	5.19 ± 2.42 (> 0.999‡)
Peritoneal	63 (< 0.001*)	132	132 (> 0.999*)	2.92 ± 2.29 (< 0.001‡)	7.33 ± 5.21	7.03 ± 4.42 (> 0.999‡)	4.27 ± 3.40 (< 0.001‡)	7.54 ± 4.56	7.24 ± 4.20 (0.565‡)
Liver	20 (< 0.001*)	45	45 (> 0.999*)	1.88 ± 1.32 (< 0.001‡)	4.20 ± 2.14	4.05 ± 1.93 (> 0.999‡)	2.78 ± 1.94 (< 0.001‡)	4.91 ± 3.68	4.69 ± 3.06 (> 0.999‡)
Bone	29 (> 0.999*)	28	28 (> 0.999*)	3.11 ± 1.14 (0.012‡)	5.00 ± 2.48	4.70 ± 2.21 (0.745)	4.68 ± 2.22 (0.009‡)	5.21 ± 2.61	4.91 ± 2.22 (> 0.999‡)
Lung	28 (> 0.999*)	28	28 (> 0.999*)	1.67 ± 0.99 (0.001‡)	3.46 ± 2.94	3.12 ± 2.70 (0.089)	2.97 ± 2.48 (< 0.001‡)	3.27 ± 3.87	3.18 ± 3.34 (0.596‡)

Data in parentheses were adjusted *P* values after Bonferroni corrections from comparisons between corresponding variables with those of PET_{D50-60}

SD standard deviation, *TLR* tumor-to-liver ratio, *TBR* tumor-to-blood ratio, PET_{FDG} [^{18}F]FDG PET, PET_{D50-60} and PET_{D30-40} dual-tracer PET reconstructed 50–60 min and 30–40 min post injection of [^{68}Ga]Ga-DOTA-FAPI-04, *LN* lymph node

*Cochran Q test

†One-way ANOVA with repeated measures

‡Freidman test

in previous studies [21–23]. Using the high-sensitivity total-body PET/CT scanner, PET imaging with reduced tracer activity as low as 10 × reduction has been previously validated [12, 24].

Although the diagnostic performance of [^{68}Ga]Ga-FAPI PET/CT could be obtained shortly after administration [2], imaging at about 60 min is still the standard method. Therefore, a 60-min dynamic [^{68}Ga]Ga-FAPI PET imaging was performed to reconstruct a static PET at 50–60 min after injection in this study, aiming to avoid a whole-body diagnostic CT scan. This protocol is different from the one reported recently by Roth et al. [9], in which [^{68}Ga]Ga-FAPI PET/CT was performed independently after [^{18}F]FDG PET/CT, although on the same day. Taking advantage of the long-AFOV PET/CT scanner wherein whole-body PET/CT can be acquired within "one bed position" [10, 11], FDG-FAPI dual-tracer PET imaging is available to be performed in a single study rather than two consequent independent studies such that two diagnostic CT scans are necessary. However, the protocol we proposed is not suitable for patients who cannot suffer from long-time immobilization. Coregistering the second PET to the first AC CT may introduce errors to the attenuation correction of the dual-tracer PET if any motion occurs during the entire examination interval. Fortunately, equal performance could be obtained 30 min after additional injection of [^{68}Ga]Ga-DOTA-FAPI-04; this may provide an alternative to these patients. In addition, this protocol is not available for evaluating metabolic response, since accurate SUVs are not measurable.

A worry for dual-tracer PET imaging may be the influence of accumulation of the first tracer to the imaging of the second tracer. This is why an ultralow activity of [^{18}F]FDG and a relatively longer time interval (84.6 ± 28.0 min) between injection and PET/CT scan were considered in this study, compared to that (55–75 min) recommended in the guideline [25]. Combined with the time interval (60 min) between [^{68}Ga]Ga-DOTA-FAPI-04 injection and static dual-tracer PET reconstruction, a total time of approximately 145 min might allow sufficient weakening of this influence, leading to the dual-tracer PET in our study more FAPI weighted than those of Roth et al. [9]. As expected, higher TNRs were identified both in primary and metastatic lesions on dual-tracer PET than [^{18}F]FDG PET. This may also be associated with the complementary nature of [^{18}F]FDG and [^{68}Ga]Ga-DOTA-FAPI-04, which target differently to tumor parenchyma and stroma, respectively. Higher detection rate of lesions, upstaging of patients, and increased diagnostic confidence were obtained with dual-tracer PET/CT than with [^{18}F]FDG PET/CT. These results were consistent with those that directly compared [^{68}Ga]Ga-FAPI PET/CT with [^{18}F]FDG PET/CT in tumor imaging [3, 5, 16]. This means the superiority of [^{68}Ga]Ga-FAPI PET over [^{18}F]FDG PET

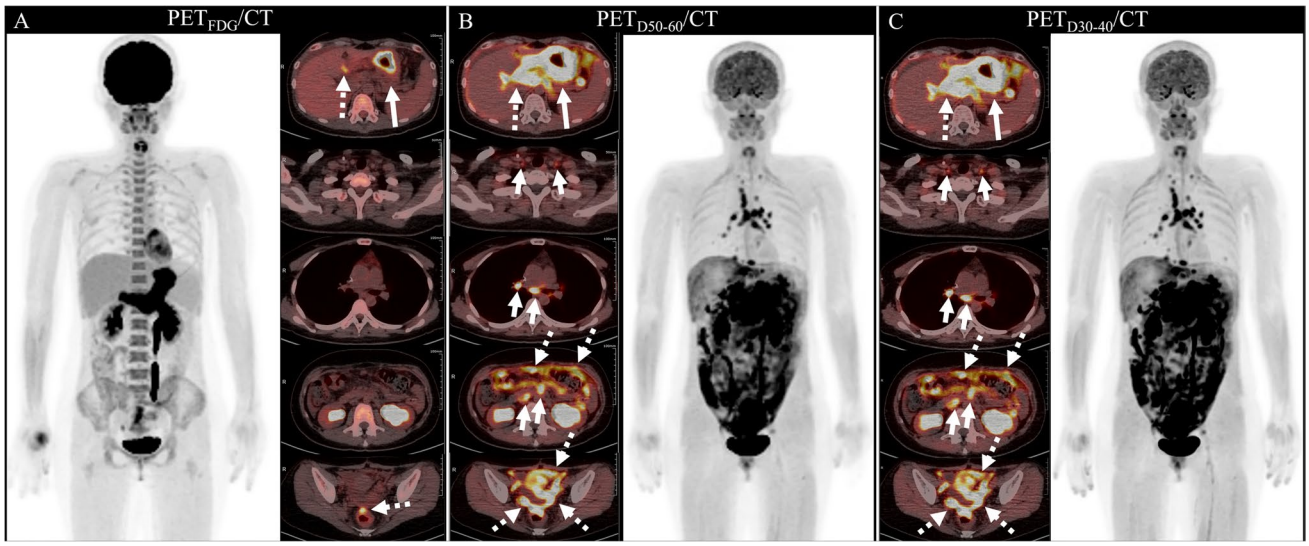

Fig. 4 A 32-year-old woman with confirmed gastric adenocarcinoma. **A** Images from [^{18}F]FDG PET/CT show obvious tracer uptake in the stomach (long arrow), accompanied by suspected peritoneal metastases (dashed arrows) in the area of hepatic hila and in the pelvic floor in front of rectum. **B** Images from dual-tracer PET$_{D50–60}$/CT demonstrate higher tracer uptake of greater extent in both primary (long arrow) and peritoneal metastases (dashed arrows) than [^{18}F]FDG PET/CT. Furthermore, multiple lymph-node metastases (short arrows) were found in multiple areas that were not visible on [^{18}F]FDG PET. **C** Images from dual-tracer PET$_{D30–40}$/CT demonstrate similar findings as PET$_{D50–60}$/CT (**B**)

and their complementary value might be obtained through a one-stop dual-tracer PET/CT scan rather than two independent studies performed on two different days. However, the increased tumor-to-background contrast on dual-tracer PET is unable to be determined to what extent by [^{18}F]FDG accumulation at a later time point and to what extent by additional [^{68}Ga]Ga-DOTA-FAPI-04 uptake. The diagnostic gain value that dual tracer has brought might be the result of complementarity between the two tracers.

The advantage of FAPI-based PET over [^{18}F]FDG PET in diagnosing various cancers may be associated with decreased background uptake leading to improved tumor contrast [26]. In the current study, the most obvious advantage of dual-tracer PET over single [^{18}F]FDG PET lies in

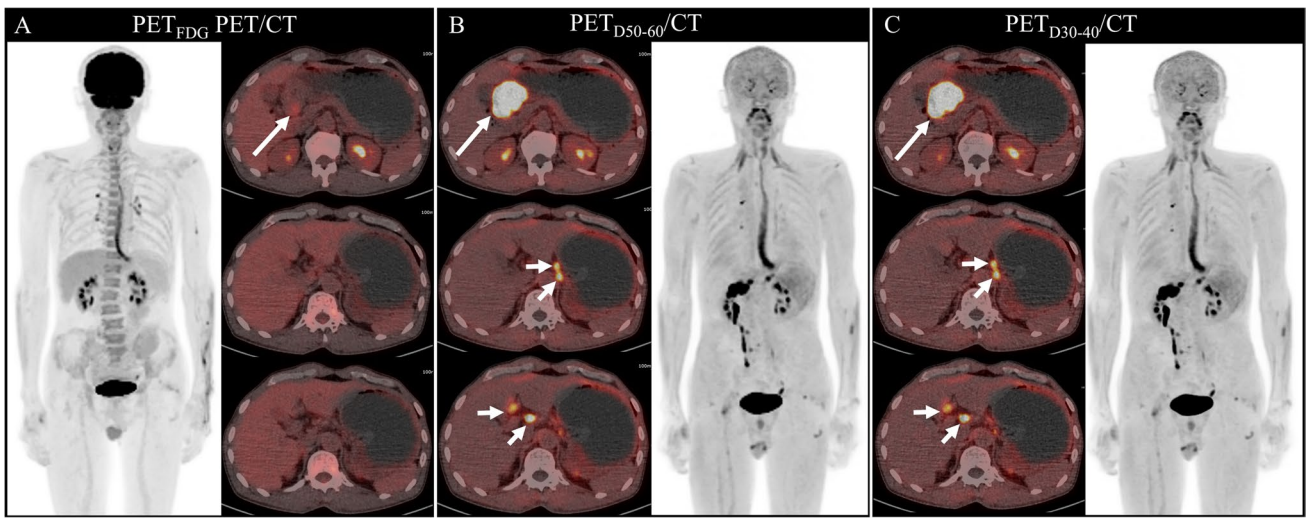

Fig. 3 Images obtained in a 66-year-old man with poorly differentiated gastric adenocarcinoma who underwent [^{18}F]FDG PET/CT (**A**) and [^{18}F]FDG/[^{68}Ga]Ga-DOTA-FAPI-04 dual-tracer PET/CT (**B** and **C**) for initial assessment. Images from [^{18}F]FDG PET/CT show slight tracer uptake in the primary tumor (long arrow in **A**) without any positive metastasis. On dual-tracer PET/CT reconstructed 50–60 min (PET$_{D50–60}$/CT, **B**) and 30–40 min (PET$_{D30–40}$/CT, **C**) post injection of [^{68}Ga]Ga-DOTA-FAPI-04, obvious higher tracer uptake with larger extent can be observed (long arrow in **B** and **C**) in the primary tumor than in [^{18}F]FDG PET/CT. In addition, couples of lymph-node metastases were identified around the stomach and in the area of hepatic hila (short arrows)

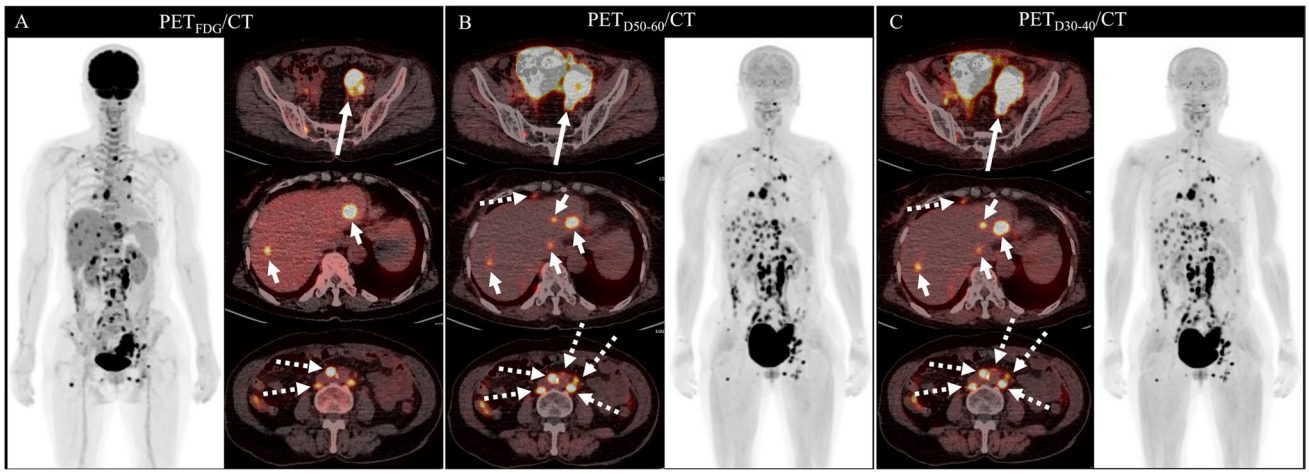

Fig. 5 A 68-year-old woman with confirmed high-grad ovarian serous carcinoma underwent PET/CT for initial assessment. **A** Images from [^{18}F]FDG PET/CT demonstrate intense tracer uptake in the left ovary (long arrow), accompanied by suspected liver metastases (short arrows) and retroperitoneal lymph-node metastases (dashed arrows). **B** Images from dual-tracer PET$_{D50-60}$/CT show equal tracer uptake as that on [^{18}F]FDG PET/CT but with larger extent (long arrow). In addition, more liver metastases (short arrows) and retroperitoneal lymph-node metastases (dashed arrows) were identified on dual-tracer PET$_{D50-60}$/CT than on [^{18}F]FDG PET/CT. **C** Images from dual-tracer PET$_{D30-40}$/CT demonstrate similar findings as PET$_{D50-60}$/CT (**B**)

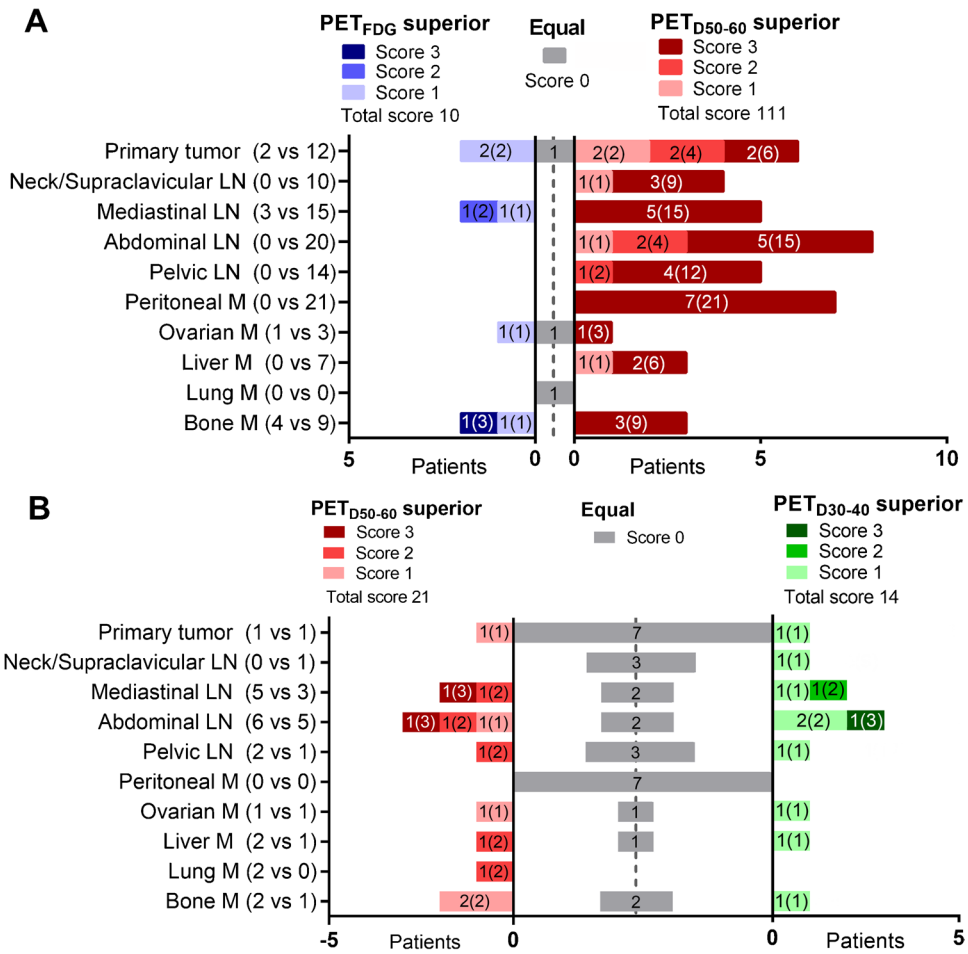

Fig. 6 Comparison of visual assessment between [^{18}F]FDG PET/CT and dual-tracer PET$_{D50-60}$/CT (**A**) and between PET$_{D50-60}$/CT and PET$_{D30-40}$/CT (**B**), wherein *n*(*n*) in each bar refers to patient number (scores). LN, lymph node; M, metastases

Table 3 Comparisons of initial staging and recurrence detection between [^{18}F]FDG PET/CT and FDG-FAPI PET/CT

A: initial staging

Type of cancer	No. of patients	PET_{FDG}/CT				$PET_{D50–60}$/CT				$PET_{D30–40}$/CT			
		I	II	III	IV	I	II	III	IV	I	II	III	IV
Gastric cancer	4	1	2[a]	0	1	0	1[a]	1	2	0	1[a]	1	2
Ovarian cancer	2	0	0	1	1	0	0	1	1	0	0	1	1
Cervical cancer	1	0	1[b]	0	0	0	1[b]	0	0	0	1[b]	0	0
Laryngeal cancer	1	0	0	1	0	0	0	1	0	0	0	1	0
Intestinal NET	1	0	1	0	0	0	1	0	0	0	1	0	0
Patients with improved staging by dual-tracer imaging						4/9 = 44.4%				4/9 = 44.4%			

B: recurrence detection

Type of cancer	No. of patients	PET_{FDG}/CT		$PET_{D50–60}$/CT		$PET_{D30–40}$/CT	
		Neg	Posi	Neg	Posi	Neg	Posi
Cervical cancer	1	0	1 (5)	0	1 (64)	0	1 (64)
Gastric cancer	1	0	1 (1)	0	1 (1)	0	1 (1)
Colon cancer	1	0	1 (1)	0	1 (1)	0	1 (1)
Appendiceal cancer	1	1	0	0	1 (2)	0	1 (2)

Clinical stage was evaluated according to the 8th edition of the American Joint Committee on Cancer staging system (reference 17). Data in parentheses are number of lesions detected

PET_{FDG} [^{18}F]FDG PET, *$PET_{D50–60}$* and *$PET_{D30–40}$* dual-tracer PET reconstructed 50–60 min and 30–40 min post injection of [^{68}Ga]Ga-DOTA-FAPI-04, *NET* neuroendocrine tumor, *Neg*. negative, *Posi*. positive

[a]One patient with gastric cancer was assigned stage IIa and IIb on [^{18}F]FDG PET/CT and dual-tracer PET/CT, respectively

[b]One patient with cervical cancer was graded stage IIa and IIb on [^{18}F]FDG PET/CT and dual-tracer PET/CT, respectively

Table 4 Radiation dosimetry of the dual-tracer imaging in comparison with those of a standard [^{18}F]FDG PET/CT imaging reported in the literatures

Studies	CT-imparted dose (mSv)	PET-related dose (mSv)			Total dose (mSv)
		[^{18}F]FDG	[^{68}Ga]Ga-FAPI	Sum	
Dual-tracer PET/CT	24.89 ± 2.37	0.43 ± 0.13	0.89 ± 0.16	1.33 ± 0.28	26.22 ± 2.57
[^{18}F]FDG PET/CT					
Reference 21	16.5–19.4	5.7–7.0	–	–	23.7–26.4
Reference 22	13.44 ± 5.44	8.19 ± 0.83	–	–	21.64 ± 5.20
Reference 23	18.56–25.95	6.23			24.79–32.18

[^{18}F]FDG 2-[^{18}F]-fluoro-2-deoxy-D-glucose, *FAPI* fibroblast activation protein inhibitor

evaluation of metastases in the lymph node and peritoneum. This may be associated with the anatomy of the peritoneum, physiological uptake of [^{18}F]FDG in the intestines, and the variable [^{18}F]FDG uptake in different tumors. As for lymph-node metastases, [^{18}F]FDG PET/CT is reported to have low sensitivity in patients with gastroenterological cancers [3, 27]. By contrast, previous studies have shown no physiological accumulation of [^{68}Ga]Ga-DOTA-FAPI-04 in the intestines, resulting in low background activity in the peritoneal cavity [3, 28]. Consistent with these previous results, the present study showed that all peritoneal and lymph-node metastases demonstrated higher TNRs with higher visual scores on dual-tracer PET. More importantly, the content of stroma was always much larger than that of tumor cells, and tumor lesions exceeding 1–2 mm in size always require formation of a supporting stroma. This suggested that stroma-targeted PET imaging may be more sensitive than glycolysis PET imaging for detecting small lesions [29], as identified in the current study. The diagnostic performance of FAPI-based PET imaging in detecting bone metastases depends on the types of primary tumor and thus remains controversial, although higher TBRs were reported by most of the previous studies on FAPI-based PET, compared to [^{18}F]FDG PET imaging [30]. Similar in the current study, the visual scoring of dual-tracer PET in detecting bone metastases was equal to [^{18}F]FDG PET, although the TLR (5.00 ± 2.8 *vs*. 3.11 ± 1.14, $P = 0.012$) and TBR (5.21 ± 2.61 *vs*. 4.68 ± 2.22, $P = 0.009$) of lesions were higher on dual-tracer PET than [^{18}F]FDG PET.

Several limitations of this work should be mentioned. First, the patient cohort is small and nearly two-thirds of patients had gastric cancers, which often demonstrate low-to-moderate

uptake of [^{18}F]FDG but high uptake of [^{68}Ga]Ga-FAPI. Therefore, the diagnostic superiority of FDG-FAPI dual-tracer PET over [^{18}F]FDG PET might be exaggerated because of substantial selection bias. The advantages of this dual-tracer protocol may not extend to patients where [^{18}F]FDG performs well as a standalone tracer (e.g., in squamous cell cancers). Second, no histological verification was possible for most of the metastatic lesions, and the work of follow-up evaluation was not performed to confirm the clinical relevance of tumor upstaging. Thus, the superiority of dual-tracer PET over [^{18}F]FDG PET could not be validated.

Conclusion

In this study, we introduced a one-stop dual-tracer, dual-low-activity imaging protocol which combines the strengths of [^{18}F]FDG and [^{68}Ga]Ga-DOTA-FAPI-04, with reduced time and radiation dosimetry. This protocol may provide an alternative approach of [^{68}Ga]Ga-DOTA-FAPI-04 PET/CT imaging supplementary to [^{18}F]FDG PET/CT in oncological imaging for appropriate patients.

Author contribution G. Liu and W. Mao had full access to all the data in the study and take responsibility for the integrity of the data and the accuracy of the data analysis. G. Liu, W. Mao, J. Gu, and H. Shi were responsible for the concept and design of the study. G. Liu, W. Mao, and H. Yu were involved in data acquisition. G. Liu and Y. Hu were involved in image review, data analysis, and interpretation. G. Liu and W. Mao drafted the manuscript, and all authors revised it critically. G. Liu and Y. Hu did the statistical analysis. J. Gu and H. Shi supervised the study. The corresponding author attests that all listed authors meet authorship criteria and that no others meeting the criteria have been omitted. J. Gu and H. Shi are the guarantors.

Funding This study was funded by the Shanghai Municipal Key Clinical Specialty Project (grant number: SHSLCZDZK03401 to H.S.), the Major Science and Technology Projects for Major New Drug Creation (grant number: 2019ZX09302001 to H.S.), the Shanghai Science and Technology Committee Program (grant number: 20DZ2201800 to H.S.), the Three-year Action Plan of Clinical Skills and Innovation of Shanghai Hospital Development Center (grant number: SHDC2020CR3079B to H.S.), and the Next Generation Information Infrastructure Construction Project founded by Shanghai Municipal Commission of Economy and Informatization (grant number: 201901014 to H.S.).

Data availability The dataset used and/or analyzed in the current study are available from the corresponding author on reasonable request.

Code availability Not applicable.

Declarations

Ethics approval This study was approved by the Ethics Committee of Zhongshan Hospital of Fudan University (approval number: B2022-098R2).

Consent to participate Written informed consents were obtained from included subjects for participation of this study.

Consent for publication The authors affirm that human research participants provided informed consent for publication of the studied data and the images in Figs. 3, 4, and 5.

Conflict of interest The authors declare no competing interests.

References

1. Kalluri R. The biology and function of fibroblasts in cancer. Nat Rev Cancer. 2016;16(9):582–98.
2. Huang R, Pu Y, Huang S, Yang C, Yang F, Pu Y, et al. FAPI-PET/CT in cancer imaging: a potential novel molecule of the century. Front Oncol. 2022;12:854658.
3. Chen H, Pang Y, Wu J, Zhao L, Hao B, Wu J, et al. Comparison of [^{68}Ga]Ga-DOTA-FAPI-04 and [^{18}F]FDG PET/CT for the diagnosis of primary and metastatic lesions in patients with various types of cancer. Eur J Nucl Med Mol Imaging. 2020;47(8):1820–32.
4. Lan L, Liu H, Wang Y, Deng J, Peng D, Feng Y, et al. The potential utility of [^{68}Ga]Ga-DOTA-FAPI-04 as a novel broad-spectrum oncological and non-oncological imaging agent—comparison with [18F]FDG. Eur J Nucl Med Mol Imaging. 2022;49(3):963–79.
5. Çermik TF, Ergül N, Yılmaz B, Mercanoğlu G. Tumor imaging with ^{68}Ga-DOTA-FAPI-04 PET/CT: comparison with 18F-FDG PET/CT in 22 different cancer types. Clin Nucl Med. 2022;47(4):e333–9.
6. Wu J, Wang Y, Liao T, Rao Z, Gong W, Ou L, et al. Comparison of the relative diagnostic performance of [^{68}Ga]Ga-DOTA-FAPI-04 and [^{18}F]FDG PET/CT for the detection of bone metastasis in patients with different cancers. Front Oncol. 2021;11:737827.
7. Peng D, He J, Liu H, Cao J, Wang Y, Chen Y. FAPI PET/CT research progress in digestive system tumours. Digest Liver Dis. 2022;54(2):164–9.
8. Qin C, Liu F, Huang J, Ruan W, Liu Q, Gai Y, et al. A head-to-head comparison of ^{68}Ga-DOTA-FAPI-04 and 18F-FDG PET/MR in patients with nasopharyngeal carcinoma: a prospective study. Eur J Nucl Med Mol Imaging. 2021;48(10):3228–37.
9. Roth KS, Voltin CA, van Heek L, Wegen S, Schomacker K, Fischer T, et al. Dual-tracer PET/CT protocol with [^{18}F]-FDG and [^{68}Ga]Ga-FAPI-46 for cancer imaging: a proof of concept. J Nucl Med. 2022;63(11):1683–6.
10. Badawi RD, Shi H, Hu P, Chen S, Xu T, Price PM, et al. First human imaging studies with the EXPLORER total-body PET scanner. J Nucl Med. 2019;60(3):299–303.
11. Alberts I, Hunermund JN, Prenosil G, Mingels C, Bohn KP, Viscione M, et al. Clinical performance of long axial field of view PET/CT: a head-to-head intra-individual comparison of the Biograph Vision Quadra with the Biograph Vision PET/CT. Eur J Nucl Med Mol Imaging. 2021;48(8):2395–404.
12. Liu G, Hu P, Yu H, Tan H, Zhang Y, Yin H, et al. Ultra-low-activity total-body dynamic PET imaging allows equal performance to full-activity PET imaging for investigating kinetic metrics of ^{18}F-FDG in healthy volunteers. Eur J Nucl Med Mol Imaging. 2021;48(8):2373–83.
13. Sui X, Liu G, Hu P, Chen S, Yu H, Wang Y, et al. Total-body PET/computed tomography highlights in clinical practice: experiences from Zhongshan Hospital. Fudan University PET Clin. 2021;16(1):9–14.

14. Yu H, Gu Y, Fan W, Gao Y, Wang M, Zhu X, et al. Expert consensus on oncological [^{18}F]FDG total-body PET/CT imaging (version 1). Eur Radiol. 2023;33(1):615–26.
15. Jacquet P, Sugarbaker PH. Clinical research methodologies in diagnosis and staging of patients with peritoneal carcinomatosis. Cancer Treat Res. 1996;82:359–74.
16. Qin C, Shao F, Gai Y, Liu Q, Ruan W, Liu F, et al. ^{68}Ga-DOTA-FAPI-04 PET/MR in the evaluation of gastric carcinomas: comparison with ^{18}F-FDG PET/CT. J Nucl Med. 2022;63(1):81–8.
17. Amin MB, Edge SB, Greene FL, Schilsky RL, Gaspar LE, Washington MK, et al. AJCC cancer staging manual (8th edition). New York: Springer; 2017.
18. ICRP. Radiation dose to patients from radiopharmaceuticals. Addendum 3 to ICRP Publication 53. ICRP Publication 106. Approved by the Commission in October 2007. Ann ICRP. 2008;38(1–2):1–197.
19. Giesel FL, Kratochwil C, Lindner T, Marschalek MM, Loktev A, Lehnert W, et al. ^{68}Ga-FAPI PET/CT: biodistribution and preliminary dosimetry estimate of 2 DOTA-containing FAP-targeting agents in patients with various cancers. J Nucl Med. 2019;60(3):386–92.
20. Christner JA, Kofler JM, McCollough CH. Estimating effective dose for CT using dose-length product compared with using organ doses: consequences of adopting International Commission on Radiological Protection publication 103 or dual-energy scanning. Am J Roentgenol. 2010;194(4):881–9.
21. Brix G, Lechel U, Glatting G, Ziegler SI, Munzing W, Muller SP, et al. Radiation exposure of patients undergoing whole-body dual-modality ^{18}F-FDG PET/CT examinations. J Nucl Med. 2005;46(4):608–13.
22. Li Y, Jiang L, Wang H, Cai H, Xiang Y, Li L. Effective radiation dose of ^{18}F-FDG PET/CT: how much does diagnostic CT contribute? Radiat Prot Dosim. 2019;187(2):183–90.
23. Huang B, Law MW, Khong PL. Whole-body PET/CT scanning: estimation of radiation dose and cancer risk. Radiology. 2009;251(1):166–74.
24. Hu Y, Liu G, Yu H, Wang Y, Li C, Tan H, et al. Feasibility of acquisitions using total-body PET/CT with an ultra-low ^{18}F-FDG activity. J Nucl Med. 2022;63(6):959–65.
25. Boellaard R, Delgado-Bolton R, Oyen WJ, Giammarile F, Tatsch K, Eschner W, et al. FDG PET/CT: EANM procedure guidelines for tumour imaging: version 2.0. Eur J Nucl Med Mol Imaging. 2015;42(2):328–54.
26. Giesel FL, Kratochwil C, Schlittenhardt J, Dendl K, Eiber M, Staudinger F, et al. Head-to-head intra-individual comparison of biodistribution and tumor uptake of ^{68}Ga-FAPI and ^{18}F-FDG PET/CT in cancer patients. Eur J Nucl Med Mol Imaging. 2021;48(13):4377–85.
27. Koerber SA, Staudinger F, Kratochwil C, Adeberg S, Haefner MF, Ungerechts G, et al. The role of ^{68}Ga-FAPI PET/CT for patients with malignancies of the lower gastrointestinal tract: first clinical experience. J Nucl Med. 2020;61(9):1331–6.
28. Kratochwil C, Flechsig P, Lindner T, Abderrahim L, Altmann A, Mier W, et al. ^{68}Ga-FAPI PET/CT: tracer uptake in 28 different kinds of cancer. J Nucl Med. 2019;60(6):801–5.
29. Calais J, Mona CE. Will FAPI PET/CT replace FDG PET/CT in the next decade?—point: an important diagnostic, phenotypic, and biomarker role. Am J Roentgenol. 2021;216(2):305–6.
30. Li L, Hu X, Ma J, Yang S, Gong W, Zhang C. A systematic review of [^{68}Ga]Ga-DOTA-FAPI-04 and [^{18}F]FDG PET/CT in the diagnostic value of malignant tumor bone metastasis. Front Oncol. 2022;12:978506.